Supplementary Information

The electrochemical and diffuse reflectance study on tetrahedral ε-Keggin-based metal-organic frameworks

Zhong-Bin Nie,[a,c] Min Zhang,[c] Tan Su,*[b,d] Liang Zhao,[c] Yuan-Yuan Wang,[c] Guang-Yan Sun*[a] and Zhong-Min Su[c]

a. Faculty of Chemistry, Yanbian University, Yanji 133002, P. R. China. E-mail: gysun@ybu.edu.cn.

b. Laboratory of Theoretical and Computational Chemistry, Institute of Theoretical Chemistry, Jilin University, Changchun 130021, P. R. China. E-mail: sutan_jlu@jlu.edu.cn.

c. Institute of Functional Material Chemistry and National & Local United Engineering Lab for Power Battery, Department of Chemistry, Northeast Normal University, Changchun 130024, P. R. China.

d. State Key Laboratory of Inorganic Synthesis and Preparative Chemistry, College of Chemistry, Jilin University, Changchun 130012, P. R. China.

S1. Materials and methods

All chemicals were purchased from commercial sources used as received without further purification. Hydrothermal syntheses of compounds **1** and **2** were carried out in 15 mL polytetrafluoroethylene lined stainless steel containers under autogenous pressure. The infrared spectra were recorded from KBr pellets in the range 4000–400 cm^{-1} using an Alpha-Centauri spectrometer. XRPD patterns were collected using a Rigaku D/max-II B X-ray diffractometer with graphite monochromatized Cu K_α radiation (λ = 1.5418 Å) and 2θ ranging from 5 to 50°. Thermogravimetric analysis (TGA) was performed using a Perkin-Elmer TG-7 analyzer in a temperature range of 20 to 700 °C under nitrogen. XPS analysis was performed on a thermo ECSALAB 250 spectrometer with an Al Kα (1486.6 eV) achromatic X-ray source running at 20 kV. The XPS binding energy (BE) was internally referenced to the aliphatic C(1s) peak (BE, 284.6 eV). The analysis of XPS data was performed using the XPS Peak Fitting Programme version 4.1. Electrochemical measurements and data collection were performed using a CHI 440 electrochemical workstation connected to a personal computer. A conventional three-electrode system was used with an Ag/AgCl electrode as the reference electrode and a Pt wire as the counter electrode. The title compounds-modified glass carbon electrodes (GCEs) were used as the working electrodes. Diffuse reflectivity was measured from 200 to 2000 nm using barium sulfate ($BaSO_4$) as a standard with 100% reflectance on a Varian Cary 500 UV-Vis spectrophotometer.

S2. Syntheses

*S2.1 Synthesis of compound **1***

A mixture of $Na_2MoO_4{\cdot}2H_2O$ (0.847 g, 3.5 mmol), molybdenum powder 99.99% (0.060 g, 0.62 mmol), H_3PO_3 (0.020 g, 0.25 mmol), zinc chloride (0.136 g, 1 mmol), CPBPC (0.238 g, 1 mmol), tetrabutylammonium hydroxide 40 wt% solution in water (120 μL, 0.18 mmol) and H_2O (7 mL) was stirred, and the pH was acidified to 5 with 2 M HCl. Then, the mixture was transferred and sealed in a Teflon-lined stainless steel autoclave at 180 °C for 3 days. After cooling to room temperature at 10 $°C{\cdot}h^{-1}$, dark-red cubic crystals suitable for X-ray diffraction study were collected after filtration (yield 35% based on H_3PO_3). Elemental analysis: Anal. Calc.: C 30.37; H 3.94; N 1.21; Mo 33.08; Zn 7.52. Found: C 30.01; H 3.65; N 1.39; Mo 33.32; Zn 7.16%.

*S2.2 Synthesis of compound **2***

A mixture of $Na_2MoO_4 \cdot 2H_2O$ (0.847 g, 3.5 mmol), molybdenum powder 99.99% (0.060 g, 0.62 mmol), H_3PO_3 (0.020 g, 0.25 mmol), zinc chloride (0.136 g, 1 mmol), TATAB (0.490 g, 1 mmol), tetrabutylammonium hydroxide 40 wt% solution in water (120 μL, 0.18 mmol) and H_2O (7 mL) was stirred, and the pH was acidified to 5 with 2 M HCl. Then, the mixture was transferred and sealed in a Teflon-lined stainless steel autoclave at 180 °C for 3 days. After cooling to room temperature at 10 °C·h^{-1}, dark-red cubic crystals suitable for X-ray diffraction study were collected after filtration (16% based on H_3PO_3). Elemental analysis: Anal. Calc.: C 29.56; H 4.17; N 5.50; Mo 30.15; Zn 6.85. Found: C 29.85; H 3.94; N 5.68; Mo 30.44; Zn 6.63%.

S3. X-ray crystallography

Single-crystal X-ray diffraction data for **1** and **2** were recorded on a Bruker ApexII CCD diffractometer with graphite-monochromated Mo K_α radiation (λ = 0.71073 Å) at 293 K. Absorption corrections were applied by using the multi-scan technique. The structures were solved by the direct method of SHELXS-97 and refined by full matrix least-squares techniques using the SHELXL-97 program within WINGX.[1-3] For compound **2**, TBA^+ cations and water molecules could not be located in the structure due to severe crystallographic disorder, and the data were corrected with SQUEEZE,[4] a part of the PLATON package of crystallographic software used to calculate the solvent molecules or counterions disorder area and to remove the contribution to the overall intensity data. The crystal data and structure refinement results of compounds **1** and **2** were summarized in Table S1.

Table S1. Crystal data and structure refinements for compounds **1** and **2**

	1	**2**
Empirical formula	$C_{88}H_{136}Mo_{12}N_3O_{50}PZn_4$	$C_{46}H_{32}Mo_{12}N_{12}O_{48}PZn_4$[a]
M_w	3479.73	2964.57
Crystal system	Orthorhombic	Monoclinic
Space group	*Pbcn*	$P2_1/c$
a (Å)	27.391(2)	31.417(3)
b (Å)	32.349(3)	19.788(2)

c (Å)	14.7330(13)	24.050(2)
α (deg)	90	90
β (deg)	90	100.334(3)
γ (deg)	90	90
V (Å^3)	13054(2)	14709(3)
Z	4	4
D_c (Mg·m^{-3})	1.770	1.339
Abs. coeff. (mm^{-1})	1.919	1.691
R_{int}	0.0825	0.0893
F(000)	6896	5660
reflns collected	94053	368233
Independent reflns	16307	26043
GOF on F^2	1.069	1.037
R_1 [$I > 2\sigma(I)$][b]	0.0714	0.0982
wR_2 [$I > 2\sigma(I)$][b]	0.1993	0.2308
R_1 (all data)[c]	0.1317	0.1147
wR_2 (all data)[c]	0.2534	0.2404

[a] The TBA^+ ions and water molecules in the crystal structure of **2** omitted for clarity. The chemical formula of compound **2** is determined as $[TBA]_3[PMo^V_8Mo^{VI}_4O_{37}(OH)_3Zn_4][PTABAB][HPTABAB]\cdot 7H_2O$.

[b] $R_1 = \Sigma||F_o| - |F_c||/\Sigma|F_o|$. [c] $wR_2 = |\Sigma w(|F_o|^2 - |F_c|^2)|/\Sigma|w(F_o^2)^2|^{1/2}$.

Table S2. The valence bond calculations for compounds **1** and **2**[5]

Compound **1**		Compound **2**			
P1	4.698	P1	4.447		
Zn1	2.001	Zn1	2.047	Zn3	1.950
Zn2	2.023	Zn2	2.079	Zn4	1.996
Mo1	5.132	Mo1	5.304	Mo7	6.011
Mo2	5.123	Mo2	5.075	Mo8	5.923
Mo3	5.975	Mo3	5.842	Mo9	4.881
Mo4	5.274	Mo4	5.848	Mo10	5.200
Mo5	5.814	Mo5	5.373	Mo11	5.274

Mo6	5.147	Mo6	5.238	Mo12	5.096
Compound **1**[a]		Compound **2**[a]			
O7	1.379	O7	1.922	O15	1.902
O8	2.098	O8	2.014	O20	1.921
O10	2.021	O9	2.021	O21	2.050
O15	2.066	O10	1.905	O22	1.995
O16	2.000	O11	1.276	O25	1.238
O19	1.403	O14	1.819	O26	2.025

[a] Only the results for μ_2-O centers of the POM units are listed in the Table.

S4. Supporting figures

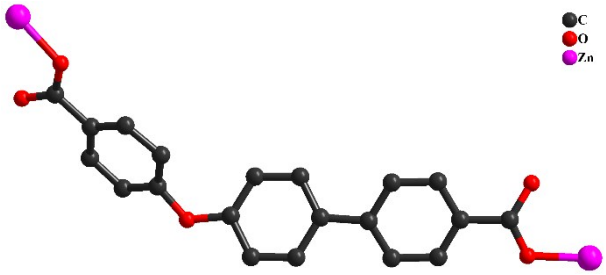

Fig. S1 The coordination mode of CPBPC fragment in compound **1**.

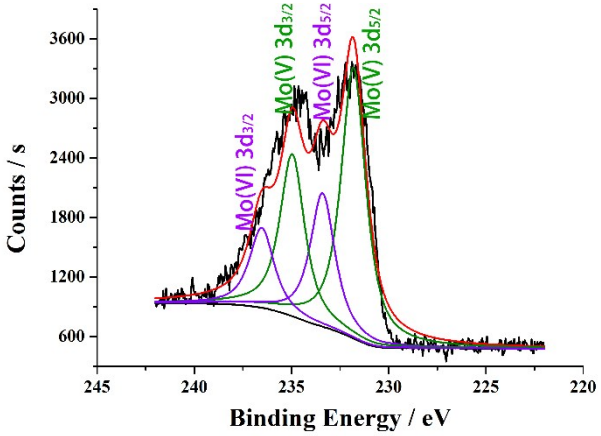

Fig. S2 The XPS analysis of Mo element in compound **1**.

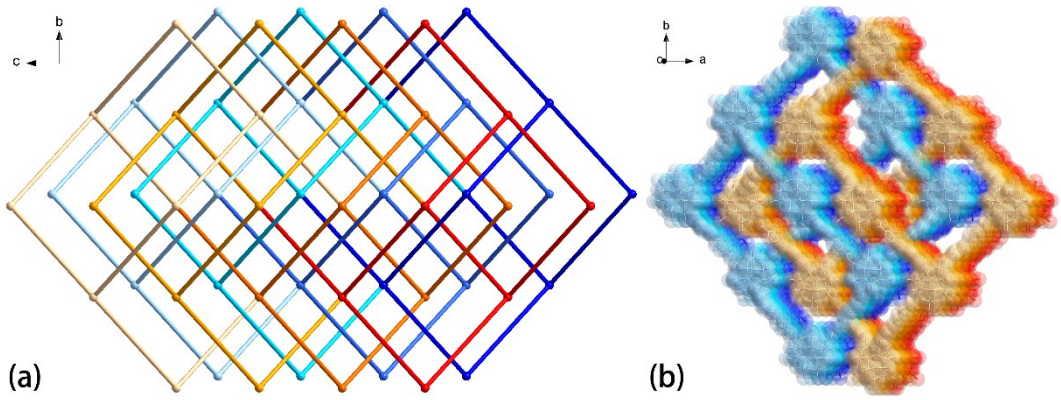

Fig. S3 The structure of **1**: (a) the 3D spacefill mode and (b) the schematic view of the [4+4] interpenetrated topology in the *a*-axis direction.

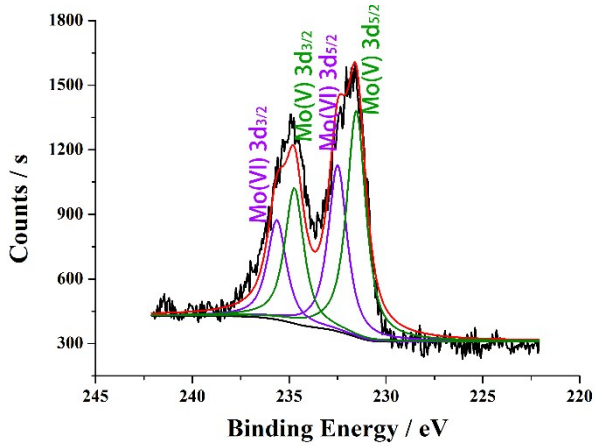

Fig. S4 The XPS analysis of Mo element in compound **2**.

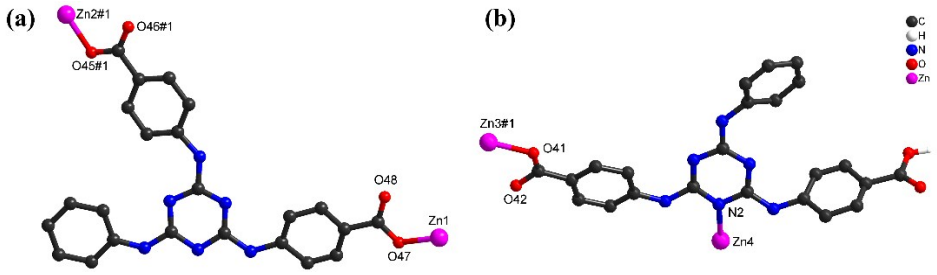

Fig. S5 The coordination modes of two distinct PTABAB fragments in compound **2**. (a) Symmetry code: #1: x, y, -1+z. (b) Symmetry code: #1: -x, -1/2+y, 1/2-z.

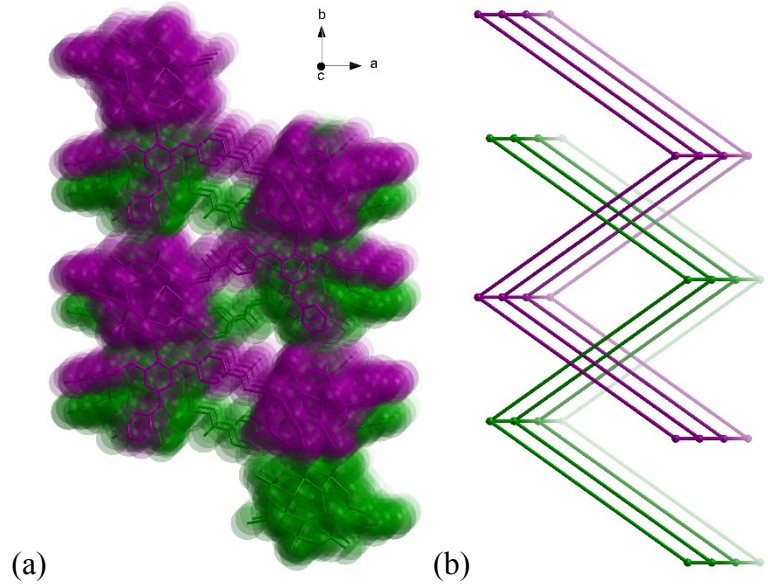

Fig. S6 The two-fold interpenetrated structure (a) and topology (b) between adjacent layers in compound **2** along the indicated dircetion.

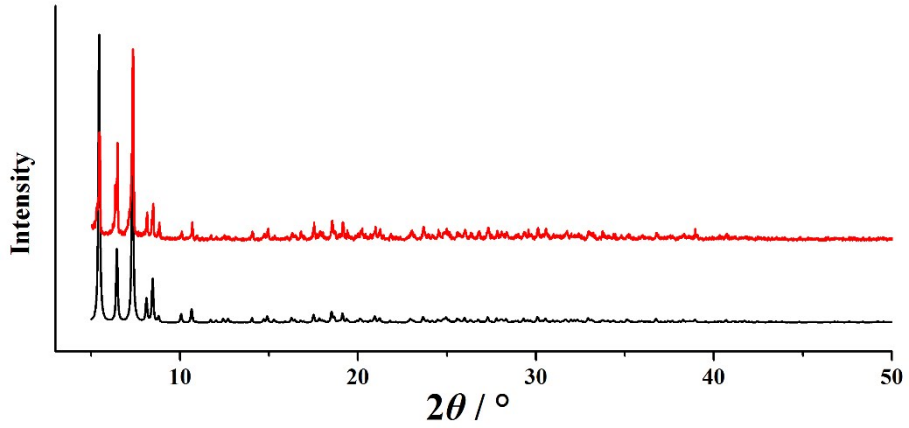

Fig. S7 The PXRD patterns of **1**: simulated pattern (*black*) and as-synthesized sample (*red*), respectively.

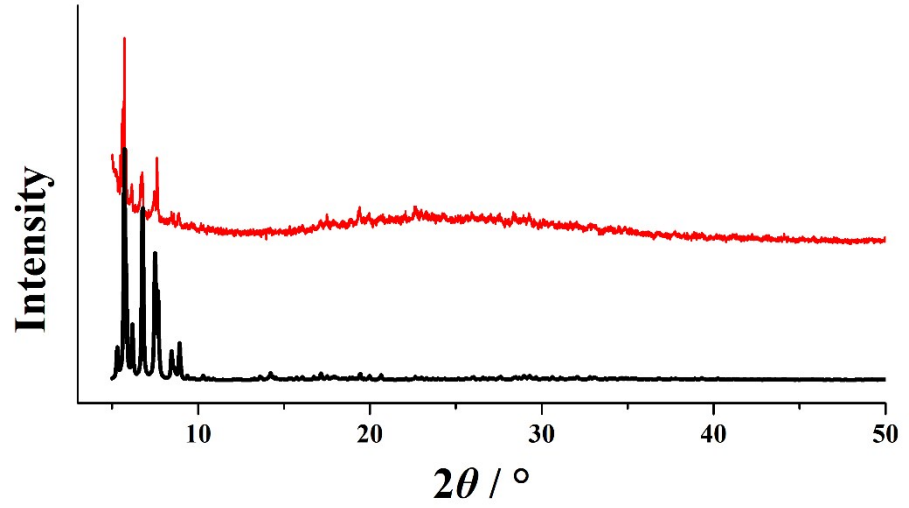

Fig. S8 The PXRD patterns of **2**: simulated pattern (*black*) and as-synthesized sample (*red*), respectively.

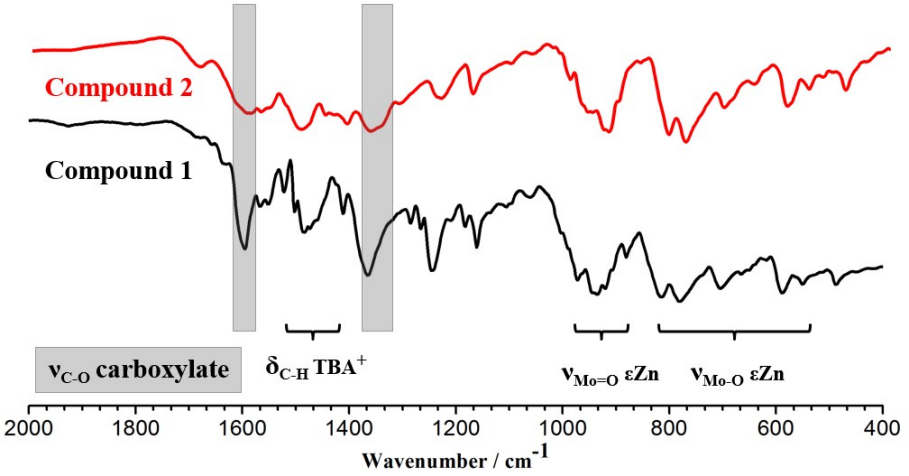

Fig. S9 The IR spectra of compounds **1** and **2** in KBr pellets.

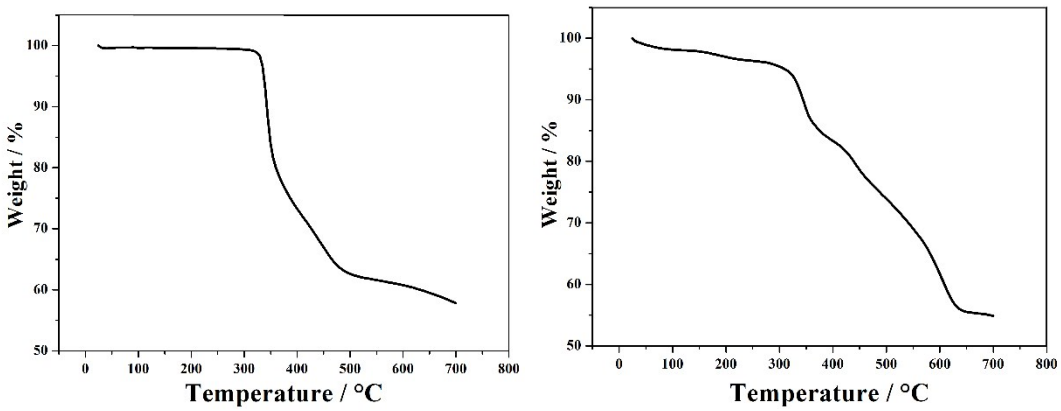

Fig. S10 The TGA curve of **1** (*left*) and **2** (*right*) measured under N_2 atmosphere from room temperature to 700 °C at a heating rate of 5 °C·min^{-1}.

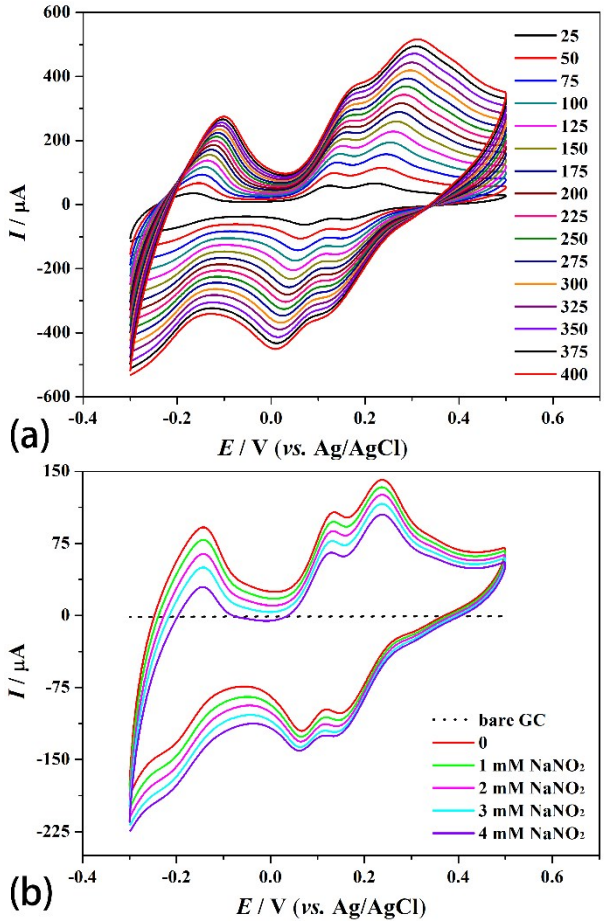

Fig. S11 The cyclic voltammograms of **1**-GCE measured in 0.1 mol·L^{-1} H_2SO_4 aqueous solution (a) at different scan rates (mV·s^{-1}) and (b) at the scan rate of 50 mV·s^{-1} containing different concentrations of $NaNO_2$, respectively.

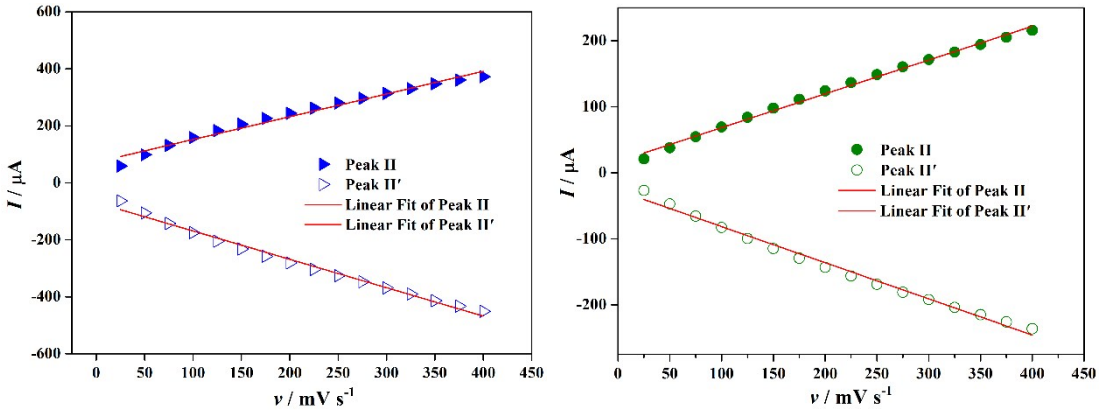

Fig. S12 The plots and linear fits of the anodic and the cathodic peaks current against scan rates for **1**- (*left*) and **2**-GCE (*right*), respectively.

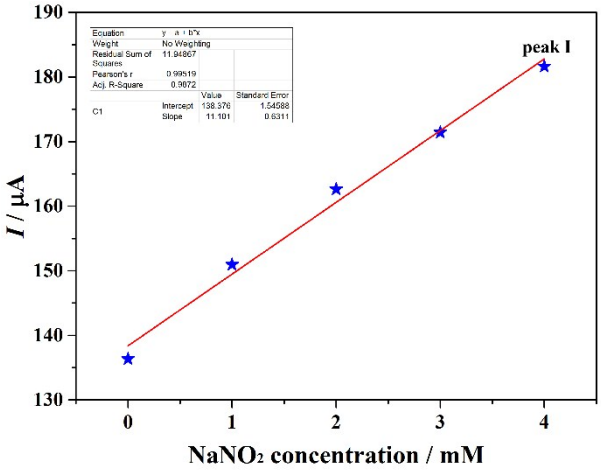

Fig. S13 The plot and linear fit of the catalytic peak currents as a function of $NaNO_2$ concentrations for **1**-GCE.

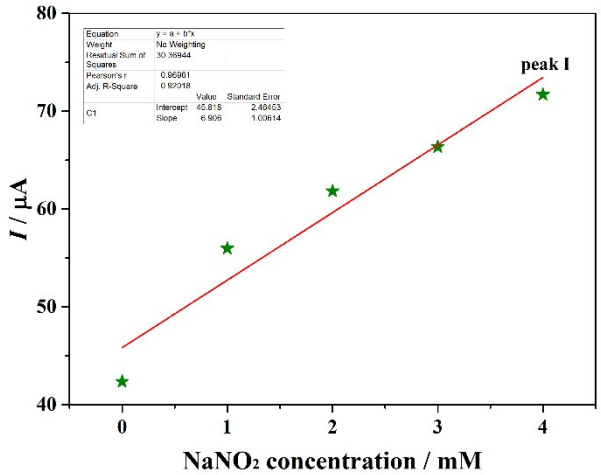

Fig. S14 The plot and linear fit of the catalytic peak currents as a function of $NaNO_2$ concentrations for **2**-GCE.

References

1 G. M. Sheldrick, *SHELXS-97*, Programs for X-ray Crystal Structure Solution, University of Göttingen: Göttingen, Germany, 1997.

2 G. M. Sheldrick, *SHELXL-97*, Programs for X-ray Crystal Structure Refinement, University of Göttingen: Göttingen, Germany, 1997.

3 L. J. Farrugia, *WINGX*, A Windows Program for Crystal Structure Analysis, University of Glasgow; Glasgow, UK, 1988.

4 P. van der Sluis and A. L. Spek, *Acta Crystallogr., Sect. A*, 1990, **46**, 194.

5 N. E. Brese and M. O'Keeffe, *Acta Cryst.*, 1991, **B47**, 192.